Letter

Parent structures of near-ambient nitrogen-doped lutetium hydride superconductor

Mingfeng Liu,[1,2,*] Xiangyang Liu,[1,*] Jiangxu Li,[1,*] Jiaxi Liu,[1,2] Yan Sun,[1] Xing-Qiu Chen,[1,†] and Peitao Liu[1,‡]
[1]*Shenyang National Laboratory for Materials Science, Institute of Metal Research, Chinese Academy of Sciences, 110016 Shenyang, China*
[2]*School of Materials Science and Engineering, University of Science and Technology of China, 110016 Shenyang, China*

(Received 11 March 2023; revised 29 May 2023; accepted 6 July 2023; published 18 July 2023)

Recently, near-ambient superconductivity has been experimentally evidenced in a nitrogen-doped lutetium hydride [Nature (London) **615**, 244 (2023)], which yields a remarkable maximum T_c of 294 K at just 10 kbar. However, due to the difficulty of x-ray diffraction (XRD) in identifying light elements, such as hydrogen and nitrogen, the crystal structure of the superconductor remains elusive, in particular, for the actual stoichiometry of hydrogen and nitrogen and their atomistic positions. This holds even for its parent structure. Here, we set out to address this issue by performing a thorough density functional theory study on the structural, electronic, dynamical, and optical properties of lutetium hydrides. Through thermal and lattice dynamic analysis as well as XRD and superconductor color comparisons, we unambiguously clarified that the parent structures are a mixture of the dominant LuH_2 phase of the CaF_2 type (instead of the originally proposed LuH_3 structure of the $Fm\bar{3}m$ space group) and the minor LuH phase of the NaCl type.

DOI: 10.1103/PhysRevB.108.L020102

Introduction. Since Onnes observed a superconducting transition on mercury in 1911 [1], the search for high-T_c superconductors at ambient conditions has been a perpetual dream for both experimental and theoretical scientists. During the past five years, boosts in the search have been witnessed in hydrogen- (H-) rich systems [2–6]. This originates from seminal intuitions of Ashcroft that room-temperature superconductors may be found in metallic hydrogen under sufficiently high pressures and hydrides at lower pressures by chemical precompression [7,8]. This results in the discovery of many hydrogen-rich superconductors that can achieve near-room-temperature superconductivity at megabar pressures, such as H_3S [9], H_3P [10], LaH_{10} [11,12], ThH_{10} [13], YH_6 [14], $YH_{9\pm x}$ [15], and Lu_4H_{23} [16].

However, the megabar pressures are still too high for practical applications. This pushes the search to the ternary and quaternary superhydrides [17–20]. Indeed, it has been theoretically predicted that the potassium-doped $Ca(BH_4)_2$ can potentially be an ambient-pressure high-T_c superconductor [21]. Very recently, near-ambient superconductivity has been experimentally evidenced in a nitrogen- (N-) doped lutetium hydride by Dasenbrock-Gammon *et al.* [22]. This is a remarkable achievement that a maximum T_c of 294 K can be achieved at a much lower pressure of 10 kbar. From a chemical perspective, the fact of the doped lutetium hydrides being high-T_c superconductors seems an natural extension of already explored yttrium- or lanthanum-superhydrides superconductors since they share similarity in the number of d and s valence electrons, i.e., lutetium (Lu) ($4f^{14}5d^16s^2$), La ($5d^16s^2$), and Y ($4d^16s^2$). In this superhydride, the N doping was claimed to play a role in providing additional carriers and suppressing the formation of H^- anions (unfavorable for superconductivity) in the lattice [22]. Nevertheless, due to the difficulty of x-ray diffraction (XRD) in identifying light elements of hydrogen and nitrogen, the crystal structure, the actual stoichiometry of hydrogen and nitrogen, as well as their atomistic positions remain elusive. This also holds for its parent structure.

In this Letter, we aim to identify the parent structures of this nitrogen-doped lutetium hydride superconductor by density functional theory (DFT) calculations. We found that simply comparing the simulated XRD to the experimental one is not capable of unequivocally determining the crystal structures: The LuH of zinc-blende type (ZB-LuH), LuH_2 of the fluorite type (FL-LuH_2), and LuH_3 in the $Fm\bar{3}m$ space group exhibit almost identical simulated XRDs that all match well the main peaks of the experimental XRD. However, $Fm\bar{3}m$-LuH_3 is thermodynamically and dynamically unstable under considered low pressures. The remaining small peaks of the experimental XRD can be well reproduced with the LuH phase of NaCl type (RS-LuH), which is dynamically stable both at 0 GPa and under pressures. Furthermore, the optical calculations show that FL-LuH_2 exhibits vanishing absorption of photons near the pink color, whereas RS-LuH and $Fm\bar{3}m$-LuH_3 show large absorption of photons near the pink color. Considering the experimentally observed pink color in the N-doped lutetium hydride superconductor samples [22], we, therefore, conclude that the dominant phase of the parent structures is most likely to be FL-LuH_2.

Computational details. The first-principles calculations were performed using the Vienna *ab initio* simulation package [24,25]. The plane-wave cutoff for the orbitals was chosen to be 500 eV. A Γ-centered k-point grid with a spacing of 0.03 $2\pi/$Å between k points was used to sample the Brillouin zone. The electronic interactions were described using the Perdew-Burke-Ernzerhof (PBE) functional [26]. The

*These authors contributed equally to this paper.
†xingqiu.chen@imr.ac.cn
‡ptliu@imr.ac.cn

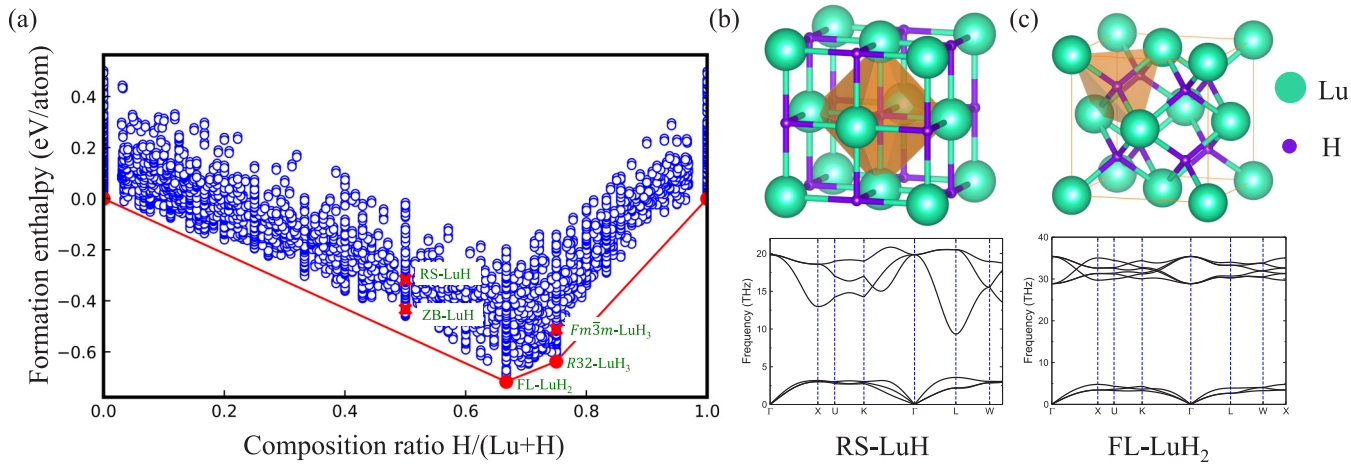

FIG. 1. (a) Calculated formation enthalpies at 1 GPa of all the structures in the Lu-H system. Each blue circle represents individual DFT computations, and the structures with the lowest formation enthalpies (in red solid circles) form a convex hull. The thermodynamical instabilities of ZB-LuH, RS-LuH, and $Fm\bar{3}m$-LuH$_3$ are indicated by red crosses. The crystal structures and phonon dispersion relationships of (b) RS-LuH and (c) FL-LuH$_2$. The polyhedral highlights the local environment of H. The detailed information on other compounds is given in the Supplemental Material [23].

projector augmented-wave pseudopotentials [27,28] with the valence electron configurations of $5p^6 5d^1 6s^2$ and $1s^1$ were employed for Lu and H, respectively. Recent theoretical studies [29,30] demonstrate that the on-site Coulomb interactions of the filled $4f$ electrons of Lu do not play any crucial role in superconductivity and stability. The Gaussian-smearing method with a smearing width of 0.05 eV was used. The convergence criteria for the total energy and ionic forces were set to 10^{-6} eV and 1 meV/Å, respectively. The variable-composition structure search was carried out using the generic evolutionary algorithm as implemented in the USPEX code [31,32] with the maximum number of atoms being set to 32. The phonon dispersion relationships were computed using a $3 \times 3 \times 3$ supercell and the PHONOPY code [33] based on density functional perturbation theory. The optical absorption spectrum was computed from the complex dielectric function, which was obtained within the independent-particle approximation [34] using dense k-point grids with a spacing of 0.01 2π/Å. Note that, here, the Drude-like contributions stemming from intraband transitions were not considered.

Structural phase diagram and phonon dispersions. Figure 1(a) shows the calculated formation enthalpies of predicted Lu-H compounds at 1 GPa derived by the variable-composition evolutionary algorithm. The structures with the lowest formation enthalpies forming a convex hull are thought to be the ground-state structures. It is evident that besides the experimentally observed FL-LuH$_2$ phase [35], a new predicted $R32$-LuH$_3$ structure with 6 Lu and 18 H atoms in the unit cell is also on the convex hull. It is interesting to note that $R32$-LuH$_3$ is an insulating phase with an indirect gap of 0.86 and 0.82 eV at 0 and 1 GPa, respectively (see Supplemental Material Figs. S1 and S2 [23]). The $Fm\bar{3}m$-LuH$_3$ is, however, above the convex hull by 86 meV/atom, indicating its thermodynamical instability. The ZB-LuH and RS-LuH are above the convex hull as well with the energies above the convex hull being 106 and 221 meV/atom, respectively. The phonon calculations demonstrate that ZB-LuH, RS-LuH, FL-LuH$_2$, and $R32$-LuH$_3$ are all dynamically stable, whereas, $Fm\bar{3}m$-LuH$_3$ exhibits soft phonon modes over the full Brillouin zone (see Fig. 1(c) and also Supplemental Material Fig. S1 [23]). We note that this is in contrast to the calculated results of Dasenbrock-Gammon *et al.* [22], which, however, showed the presence of soft modes in RS-LuH. We argue that their incorrect predictions likely originated from their less accurate computational setups. In our case, using a smaller $2 \times 2 \times 2$ supercell for RS-LuH, we also obtained the soft modes. All the detailed information on space groups, formation enthalpies, optimized lattice parameters, and the Wyckoff positions of predicted Lu-H binary compounds is given in Supplemental Material Table S1 [23]. As compared to FL-LuH$_2$, an additional hydrogen atom appears in a hollow octahedral site of $Fm\bar{3}m$-LuH$_3$ (see Supplemental Material Fig. S1 [23]), implying strong anharmonicity. Therefore, the dynamical stability of $Fm\bar{3}m$-LuH$_3$ should be further carefully examined with beyond harmonic approximation. Indeed, the phase diagram changes upon pressure, and many new LuH$_x$ phases emerge at high pressures [36–38]. For instance, $Fm\bar{3}m$-LuH$_3$ becomes thermodynamically and dynamically stable above 25 GPa [36,37,39] (also see Supplemental Material Fig. S3 [23]) and turns out to be superconducting with a $T_c = 12 \sim 15$ K under high pressures (110–170 GPa) [38]. Increasing the temperature was found to also favor the stability of $Fm\bar{3}m$-LuH$_3$ [40]. However, the predicted T_c is less than the stability temperature, indicating that $Fm\bar{3}m$-LuH$_3$ would decompose into a different structure before it has the chance to become a superconductor [40]. To summarize this section, the originally proposed $Fm\bar{3}m$-LuH$_3$ by Dasenbrock-Gammon *et al.* [22] is unlikely to be the parent structure of the superconducting sample.

XRD simulations. Figure 2 compares the simulated XRDs of different Lu-H binary compounds to the experimental one obtained at 0 GPa. One can see that ZB-LuH, FL-LuH$_2$, and $Fm\bar{3}m$-LuH$_3$ exhibit almost indistinguishable simulated XRDs that all match well the main peaks of the experimental one. This is not unexpected because all of them show the similar lattice constants ($\sim$5.0 Å) (see Supplemental

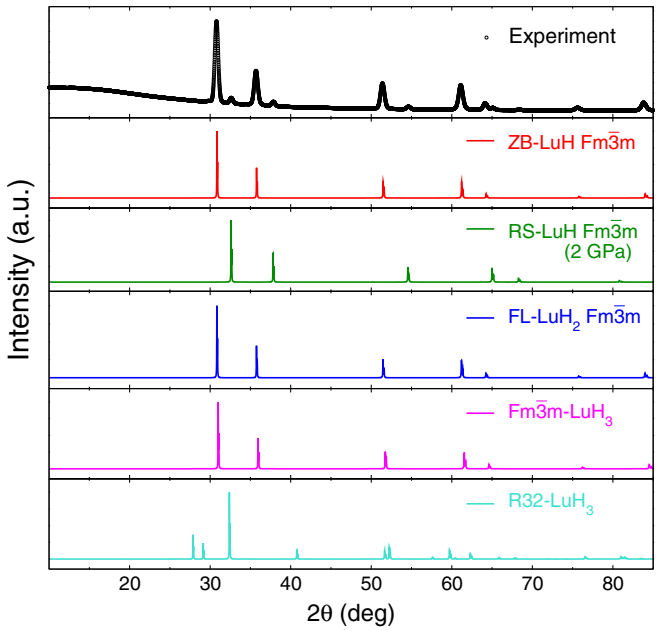

FIG. 2. Simulated XRDs of different Lu-H binary compounds at 0 GPa (except for RS-LuH, which was obtained at 2 GPa) and compared to the experimental one obtained at 0 GPa. The experimental data are taken from Ref. [22].

Material Tables S1 and S2 [23]) and the same framework of Lu (see Supplemental Material Fig. S1 [23]), whereas, the subtle differences in the number and positions of H atoms are not capable to be captured by the XRD technique. Although the $R32$-LuH$_3$ phase is the thermodynamical ground state (on the convex hull), its simulated XRD obviously deviates the experimental one, excluding its existence in the N-doped lutetium hydride superconductor. The remaining small peaks appearing in the experimental XRD can be well captured by the RS-LuH phase, indicating the existence of a small portion of the RS-LuH phase in the superconductor samples. Note that a small amount of RS-LuH also appears in recently synthesized samples of lutetium polyhydride superconductor Lu_4H_{23} [16]. It should be mentioned that the perfect agreement on the small peaks of the experimental data at 0 GPa can only be achieved by the RS-LuH phase at 2 GPa. Reducing the pressure results in increasing lattice constants, which lead to a rigid shift toward smaller diffraction angles. One might think that this is a result of the overestimation of lattice constants by the PBE functional. Indeed, using the PBEsol functional yields a better description of the lattice constant for RS-LuH (4.722 Å) than PBE (4.800 Å) as compared to the experimental one for the so-called compound B (4.753 Å [22]).

Optical spectra. Figure 3 displays the calculated optical absorption spectra of ZB-LuH, RS-LuH, FL-LuH$_2$, and $Fm\bar{3}m$-LuH$_3$ compounds at 1 GPa within the independent-particle approximation. It is evident that only FL-LuH$_2$ exhibits vanishing absorption coefficients of photons near the pink color, in good agreement with the experimental spectra [41]. This arises from the existence of large direct band gaps (∼1.9 eV) between the bands close to the Fermi level over the full Brillouin zone (see Supplemental Material Fig. S2 [23]). We note that our prediction on the pink color of FL-LuH$_2$ under pressure has been well supported by a recent experimental study [42]. By contrast, the $Fm\bar{3}m$-LuH$_3$ structure shows strong absorption of the photons near the pink color. Considering the experimentally observed pink color in the N-doped lutetium hydride superconductor samples [22], the dominant phase of the parent structures is most likely to be FL-LuH$_2$ rather than the originally proposed $Fm\bar{3}m$-LuH$_3$ structure [22]. We note that the overall optical absorption spectra change only slightly with the pressure from 0 to 1 GPa (compare Supplemental Material Fig. S1 and Fig. S2 [23]). Our Letter provides a new route to identify the parent structures via the optical spectroscopy.

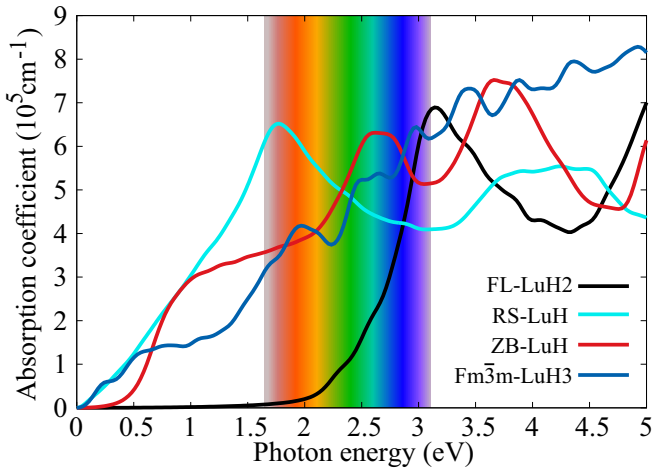

FIG. 3. Calculated optical absorption spectra of ZB-LuH, RS-LuH, FL-LuH$_2$, and $Fm\bar{3}m$-LuH$_3$ compounds at 1 GPa.

Conclusions. To summarize, we have carried out a thorough density functional theory study on the crystal structures, thermodynamic, and dynamical stabilities, as well as optical absorption spectra of lutetium hydrides. The results are summarized in Table I. It is obvious that the FL-LuH$_2$ phase is the only one that satisfies all the necessary requirements toward the experimental observations, i.e., thermodynamically and dynamically stable, no absorption of pink-color photons, and matching well the main peaks of the experimental XRD. Therefore, we can conclude that the FL-LuH$_2$ phase is the dominant phase of the parent structures of the recently experimentally synthesized near-ambient high-T_c lutetium hydride superconductor. Our prediction has later been confirmed by many experimental works [42–45] that all rely on FL-LuH$_2$.

TABLE I. A summary of energy above the convex hull ($E_{\rm hull}$, in meV/atom), phonon stability, and absorption of the pink-color photons as well as matching degree on the experimental XRD for different Lu-H binary compounds at 1 GPa.

Phase	$E_{\rm hull}$	Phonon stability	Absorption of pink-color photons	XRD match
ZB-LuH	106	Yes	Yes	Dominant peaks
RS-LuH	221	Yes	Yes	Minor peaks
FL-LuH$_2$	0	Yes	No	Dominant peaks
$Fm\bar{3}m$-LuH$_3$	86	No	Yes	Dominant peaks
$R32$-LuH$_3$	0	Yes	No	No match

The remaining small peaks of the experimental XRD can better be described by the existence of a small portion of the RS-LuH phase, which is phonon stable at 0 GPa and under pressures. This is further confirmed by the fact that the predicted lattice constants for FL-LuH_2 (5.017 Å) and RS-LuH (4.800 Å) at 0 GPa agree well with the experimental values (5.029 and 4.753 Å for the so-called compound A and compound B, respectively) [22]. Given the unambiguous identification of the parent structures, it is time to study the role of nitrogen doping in this near-ambient high-T_c lutetium hydride superconductor. It is interesting to note that, the LuH_2 phase is nonsuperconducting as predicted by electron-phonon calculations [22] and confirmed by a recent experimental work [42]. Even with N doping in LuH_2, recent experiments demonstrated the absence of superconductivity [43,45]. Recent theoretical studies [29,30,46,47] do not obtain thermodynamically stable Lu-H-N ternary phases at 0 K and ambient pressures. Theoretical attempts to calculate T_c in the Lu-H-N system within the conventional BCS theory of superconductivity have found values of T_c two orders of magnitude smaller [29,30] than reported by Dasenbrock-Gammon *et al.* [22]. Therefore, whether the proposed near-ambient superconductivity in a N-doped lutetium hydride is true or an experimental artifact remains to be clarified.

Note added in proof. Recently, we became aware of a similar work [48] that confirms our conclusion.

Acknowledgments. This work was supported by the National Key R&D Program of China (Grant No. 2021YFB3501503), the National Science Fund for Distinguished Young Scholars (Grant No. 51725103), and Chinese Academy of Sciences (Grant No. ZDRW-CN-2021-2-5). All calculations were performed on the high performance computational cluster at the Shenyang National University Science and Technology Park.

[1] H. K. Onnes, Commun. Phys. Lab. Univ. Leiden **12**, 120 (1911).
[2] J. Lv, Y. Sun, H. Liu, and Y. Ma, Matter Radiat. Extremes **5**, 068101 (2020).
[3] J. A. Flores-Livas, L. Boeri, A. Sanna, G. Profeta, R. Arita, and M. Eremets, Phys. Rep. **856**, 1 (2020).
[4] D. V. Semenok, I. A. Kruglov, I. A. Savkin, A. G. Kvashnin, and A. R. Oganov, Curr. Opin. Solid State Mater. Sci. **24**, 100808 (2020).
[5] X. Zhang, Y. Zhao, F. Li, and G. Yang, Matter Radiat. Extremes **6**, 068201 (2021).
[6] B. Lilia, R. Hennig, P. Hirschfeld, G. Profeta, A. Sanna, E. Zurek, W. E. Pickett, M. Amsler, R. Dias, M. I. Eremets, C. Heil, R. J. Hemley, H. Liu, Y. Ma, C. Pierleoni, A. N. Kolmogorov, N. Rybin, D. Novoselov, V. Anisimov, A. R. Oganov *et al.*, J. Phys.: Condens. Matter **34**, 183002 (2022).
[7] N. W. Ashcroft, Phys. Rev. Lett. **21**, 1748 (1968).
[8] N. W. Ashcroft, Phys. Rev. Lett. **92**, 187002 (2004).
[9] A. P. Drozdov, M. I. Eremets, I. A. Troyan, V. Ksenofontov, and S. I. Shylin, Nature (London) **525**, 73 (2015).
[10] A. P. Drozdov, M. I. Eremets, and I. A. Troyan, arXiv:1508.06224.
[11] A. P. Drozdov, P. P. Kong, V. S. Minkov, S. P. Besedin, M. A. Kuzovnikov, S. Mozaffari, L. Balicas, F. F. Balakirev, D. E. Graf, V. B. Prakapenka, E. Greenberg, D. A. Knyazev, M. Tkacz, and M. I. Eremets, Nature (London) **569**, 528 (2019).
[12] M. Somayazulu, M. Ahart, A. K. Mishra, Z. M. Geballe, M. Baldini, Y. Meng, V. V. Struzhkin, and R. J. Hemley, Phys. Rev. Lett. **122**, 027001 (2019).
[13] D. V. Semenok, A. G. Kvashnin, A. G. Ivanova, V. Svitlyk, V. Y. Fominski, A. V. Sadakov, O. A. Sobolevskiy, V. M. Pudalov, I. A. Troyan, and A. R. Oganov, Mater. Today **33**, 36 (2020).
[14] I. A. Troyan, D. V. Semenok, A. G. Kvashnin, A. V. Sadakov, O. A. Sobolevskiy, V. M. Pudalov, A. G. Ivanova, V. B. Prakapenka, E. Greenberg, A. G. Gavriliuk, I. S. Lyubutin, V. V. Struzhkin, A. Bergara, I. Errea, R. Bianco, M. Calandra, F. Mauri, L. Monacelli, R. Akashi, and A. R. Oganov, Adv. Mater. **33**, 2006832 (2021).
[15] E. Snider, N. Dasenbrock-Gammon, R. McBride, X. Wang, N. Meyers, K. V. Lawler, E. Zurek, A. Salamat, and R. P. Dias, Phys. Rev. Lett. **126**, 117003 (2021).
[16] Z. Li, X. He, C. Zhang, K. Lu, B. Bin, J. Zhang, S. Zhang, J. Zhao, L. Shi, S. Feng, X. Wang, Y. Peng, R. Yu, L. Wang, Y. Li, J. Bass, V. Prakapenka, S. Chariton, H. Liu, and C. Jin, Sci. China Phys., Mech. Actron. **66**, 267411 (2023).
[17] Y. Sun, J. Lv, Y. Xie, H. Liu, and Y. Ma, Phys. Rev. Lett. **123**, 097001 (2019).
[18] S. Di Cataldo, W. von der Linden, and L. Boeri, Phys. Rev. B **102**, 014516 (2020).
[19] N. Geng, T. Bi, and E. Zurek, J. Phys. Chem. C **126**, 7208 (2022).
[20] A. D. Grockowiak, M. Ahart, T. Helm, W. A. Coniglio, R. Kumar, K. Glazyrin, G. Garbarino, Y. Meng, M. Oliff, V. Williams, N. W. Ashcroft, R. J. Hemley, M. Somayazulu, and S. W. Tozer, Front. Electron. Mater. **2**, 837651 (2022).
[21] S. Di Cataldo and L. Boeri, Phys. Rev. B **107**, L060501 (2023).
[22] N. Dasenbrock-Gammon, E. Snider, R. McBride, H. Pasan, D. Durkee, N. Khalvashi-Sutter, S. Munasinghe, S. E. Dissanayake, K. V. Lawler, A. Salamat, and R. P. Dias, Nature (London) **615**, 244 (2023).
[23] See Supplemental Material at http://link.aps.org/supplemental/10.1103/PhysRevB.108.L020102 for the detailed information on crystal structures, phonon dispersion relationships, electronic band structures, and optical absorption spectra of the Lu-H binary compounds.
[24] G. Kresse and J. Hafner, Phys. Rev. B **47**, 558 (1993).
[25] G. Kresse and J. Furthmüller, Phys. Rev. B **54**, 11169 (1996).
[26] J. P. Perdew, K. Burke, and M. Ernzerhof, Phys. Rev. Lett. **77**, 3865 (1996).
[27] P. E. Blöchl, Phys. Rev. B **50**, 17953 (1994).
[28] G. Kresse and D. Joubert, Phys. Rev. B **59**, 1758 (1999).
[29] P. P. Ferreira, L. J. Conway, A. Cucciari, S. D. Cataldo, F. Giannessi, E. Kogler, L. T. F. Eleno, C. J. Pickard, C. Heil, and L. Boeri, arXiv:2304.04447.
[30] K. P. Hilleke, X. Wang, D. Luo, N. Geng, B. Wang, and E. Zurek, arXiv:2303.15622 [Phys. Rev. B (to be published)].
[31] A. R. Oganov and C. W. Glass, J. Chem. Phys. **124**, 244704 (2006).
[32] A. O. Lyakhov, A. R. Oganov, H. T. Stokes, and Q. Zhu, Comput. Phys. Commun. **184**, 1172 (2013).
[33] A. Togo and I. Tanaka, Scr. Mater. **108**, 1 (2015).

[34] M. Gajdoš, K. Hummer, G. Kresse, J. Furthmüller, and F. Bechstedt, Phys. Rev. B **73**, 045112 (2006).
[35] J. E. Bonnet and J. N. Daou, J. Appl. Phys. **48**, 964 (1977).
[36] H. Xie, Y. Yao, X. Feng, D. Duan, H. Song, Z. Zhang, S. Jiang, S. A. T. Redfern, V. Z. Kresin, C. J. Pickard, and T. Cui, Phys. Rev. Lett. **125**, 217001 (2020).
[37] H. Song, Z. Zhang, T. Cui, C. J. Pickard, V. Z. Kresin, and D. Duan, Chin. Phys. Lett. **38**, 107401 (2021).
[38] M. Shao, S. Chen, W. Chen, K. Zhang, X. Huang, and T. Cui, Inorg. Chem. **60**, 15330 (2021).
[39] Y. Sun, F. Zhang, S. Wu, V. Antropov, and K.-M. Ho, Phys. Rev. B **108**, L020101 (2023).
[40] R. Lucrezi, P. P. Ferreira, M. Aichhorn, and C. Heil, arXiv:2304.06685.
[41] J. H. Weaver, R. Rosei, and D. T. Peterson, Phys. Rev. B **19**, 4855 (1979).
[42] P. Shan, N. Wang, X. Zheng, Q. Qiu, Y. Peng, and J. Cheng, Chin. Phys. Lett. **40**, 046101 (2023).
[43] X. Ming, Y.-J. Zhang, X. Zhu, Q. Li, C. He, Y. Liu, B. Zheng, H. Yang, and H.-H. Wen, Nature (London) (2023), doi:10.1038/s41586-023-06162-w.
[44] Y.-J. Zhang, X. Ming, Q. Li, X. Zhu, B. Zheng, Y. Liu, C. He, H. Yang, and H.-H. Wen, Sci. China: Phys. Mech. Astron. **66**, 287411 (2023).
[45] X. Xing, C. Wang, L. Yu, J. Xu, C. Zhang, M. Zhang, S. Huang, X. Zhang, B. Yang, X. Chen, Y. Zhang, J.-g. Guo, Z. Shi, Y. Ma, C. Chen, and X. Liu, arXiv:2303.17587.
[46] F. Xie, T. Lu, Z. Yu, Y. Wang, Z. Wang, S. Meng, and M. Liu, Chin. Phys. Lett. **40**, 057401 (2023).
[47] Z. Huo, D. Duan, T. Ma, Q. Jiang, Z. Zhang, D. An, F. Tian, and T. Cui, Matter Radiat. Extremes **8**, 038402 (2023).
[48] X. Tao, A. Yang, S. Yang, Y. Quan, and P. Zhang, Sci. Bull. (2023), doi:10.1016/j.scib.2023.06.007.